An Adaptive Video Data Representation Model to Increase Delivery Efficiency in Next-Generation Networks

Anton Sorokun[1], Yurii Zadontsev[1], Dmytro Chyrva[2], Mykyta Zhyzhkin[2], and Andrii Bondarenko[1]

[1]*State University of Information and Communication Technologies, Kyiv, Ukraine,*
[2]*State University "Kyiv Aviation Institute", Kyiv, Ukraine*

https://doi.org/10.26636/jtit.2026.1.2411

Abstract — This study proposes an adaptive video stream representation model that provides dynamic adjustment of bitrate, frame rate, compression ratio, and frame structure based on a comprehensive analysis of network conditions, content priorities, and technical features of endpoint equipment. The research methodology includes mathematical modeling of video data transmission processes, analysis of radio channel noise immunity, algorithmic formalization of adaptive optimization of video parameters, and simulation modeling in Wi-Fi, 4G/5G, and PON networks. The results show that the proposed model provides a bandwidth reduction of 22 – 30% compared to static coding and classical ABR algorithms, reduces buffer time by 40 – 60%, increases delay stability to 150 ms in 5G and to 300 ms in 4G networks, and decreases packet loss rate to 1 – 3%. Its PSNR and SSIM metrics remain stable and device load is reduced by 15 – 20%.

Keywords — adaptive video data representation, channel modeling, next-generation networks, noise immunity, quality of experience, video stream optimization

1. Introduction

Modern telecommunication technologies, such as 5G and 6G networks, as well as widespread use of Wi-Fi 6/7 standards, caused an exponential growth in the transmission of video content. This growth is driven by the emergence and mass popularization of ultra-high resolution (4K/8K) applications and services, transmission of augmented and virtual reality (AR/VR) information, telemedicine and distance learning systems, and the Internet of Things (IoT), including narrowband solutions [1]. In all those applications, quality of experience (QoE) is of key importance for media-related services.

However, despite the increased capacity and reduced delay of next-generation networks, numerous fundamental problems remain that can impede efficient and stable video data delivery [2]. These include high volatility of wireless channel capacity, which can be caused by fading, interference, and user mobility, significant transmission delays and jitter, and possible packet loss during transmission. Limitation of computing resources and power consumption constraints affecting massive end-devices may be experienced as well.

Current, commonly used approaches to solving these problems demonstrate good effectiveness when relying on HTTP-based and adaptive streaming (AVR), software-defined networking (SDN), network function virtualization (NFV) and edge computing (EC) technologies. However, as current research shows, existing solutions may be based on client-side adaptation or direct routing optimization that does not skips, skip with errors or delays, a holistic model that could dynamically adapt the most fundamental representation of video data based on a comprehensive analysis of the network state and equal transmission of all characteristics of the content [3].

Hence, a problem arises of developing an adaptive video data representation model that would be capable of optimizing the parameters of a video stream at all stages of its life cycle, under the conditions of constantly evolving and dynamically changing new generation networks.

In this context, this research aims to develop an adaptive video data representation model to improve the efficiency and reliability of video content delivery (streaming) in 5G/6G, Wi-Fi, and NB-IoT networks through multi-parameter structured optimizations of video stream parameters in real time.

To achieve this goal, the following research objectives are formulated.

- analysis of current literature regarding the methods and technologies for adapting video streams, as well as identification of their advantages and disadvantages in new generation networks,
- development of an architecture of the adaptive video data representation model, which may include mechanisms for monitoring network status, classifying types of end devices, and analyzing video content priorities;
- identification of hybrid adaptation algorithms that provide dynamic adjustment of key video stream parameters based on incoming data,
- analysis of the developed model to evaluate its effectiveness based on key metrics.

The scientific novelty consists in the creation of an adaptive video data representation model that is immune to noise. Integration of dynamic bitrate control, frequency filtering, and

energy-saving mechanisms provides comprehensive stabilization of the video stream in the case of bandwidth fluctuations with regular or quasiregular components. This makes the developed model a promising solution for 5G/6G networks, where video quality is one of the key technological priorities.

2. Literature Review

The current stage of the development of telecommunication networks is characterized by the transition from 3G and 4G technologies to 5G networks, as well as by preparation for the advent of 6G networks. This process creates increased requirements for the efficiency and speed of video content delivery [2]. Growing traffic volumes, the emergence of new services and applications, and the need to ensure stable QoE require a revision of traditional approaches to video transmission. Current research identifies promising areas for solving these problems and offers technological solutions that can optimize video content transmission in the context of the development of new generation networks [4].

One of the current research areas is the development of fundamental technologies for video delivery over modern networks using adaptive bitrate streaming rate (ABR). Paper [5] covers the full scope of modern achievements and the next research vectors, showing the evolution from the simplest adaptive bitrate selection to intelligent systems that can take into account the network component, its state, content characteristics, and QoE. Another trend is the use of AI to optimize ABR, as demonstrated in [6], [7], where the benefits and effectiveness of the deep reinforcement learning (DRL) technique are relied upon.

These approaches enable bandwidth prediction, and thus allow for adaptation of video quality and maximization of QoE. Article [8] supports this idea by proposing a machine learning-based packet switching path for stabilization and the ability to transmit multiple video streams, which will be needed by companies broadcasting mass events.

The architectural shifts and computing frontiers are also highlighted by the authors of [9], who claim that the transition to next-generation networks is not possible without SDN, NFV, and EC. Article [10] stated that the combination of SDN and NFV plays a key part in ensuring QoE in ultra-advanced 6G networks. It emphasizes the importance of close and joint integration between the physical layer of a 6G network and the data presentation layer.

Furthermore, in [11] a reliable physical and link layer is created to optimize payload for video transmission over LoRa using HARQ. This direction was also considered in [12]. In terms of capacity planning in NOMA networks, the authors solve the problem of efficient resource utilization in the face of limited bandwidth, interference and obstacles.

Furthermore, the structural and selective methods described by the authors of [13] provide an alternative view of adaptive video representation by focusing on selective frame processing and the extraction of key components. They display efficient coding of structural components and segments of video frames with key information requirements. In [14], methods for motion compensation and syntactic data representation are developed. The developments aim to reduce bitrate redundancy through intelligent analysis of the content structure (video content), which is an important addition to conventional standard codes.

In [15], [16], the effect of non-fluctuating and multipath interference on signal immunity under conditions of limited bandwidth and interference during multiposition phase manipulation is analyzed. The results obtained serve as a basis for building more accurate models of the communication channel which, in turn, ensure the effective operation of adaptive upper-level algorithms [17].

In addition, the authors of [18] demonstrate that taking into account non-fluctuation components facilitates obtaining more accurate channel quality predictions. Article [19] proposes an integrated approach to group recommendation, caching, and video transmission in the IoT for smart transportation, which is also based on machine learning methods.

Papers [20], [21] focus on probabilistic caching and routing algorithms for video data in dense device-to-device (D2D) networks and VANETs, respectively. Using roadside units (RSUs) and DRL techniques, the research demonstrates that efficient video delivery in such networks requires not only client-side adaptation, but also intelligent resource allocation throughout the network.

Despite the progress in adaptive algorithms, the efficiency of video data processing remains a fundamental factor. Two approaches can be distinguished here. The first is presented in [22], where structural and selective coding methods are developed. The other is presented in [23], where the latest codecs and communication technologies are described. The authors emphasize the need to optimize coding algorithms to ensure high-quality video content transmission in next-generation networks.

To ensure end-to-end adaptation of the video delivery process from bitrate selection to caching at the network edge, it is necessary to use AI technologies, primarily DRL methods. Moreover, there is a need to establish an architectural imperative, i.e., to create solutions that will be closely integrated with SDN/NFV and MEC paradigms. In addition, analysis of the literature shows a lack of comprehensiveness of existing research: most studies focus only on certain aspects (client-side adaptation, server caching, or coding methods). Simultaneously, not all papers propose a holistic video data representation model capable of ensuring adaptability at all content lifecycle stages.

In this regard, a promising direction is to combine efficient coding structural methods with intelligent adaptation algorithms (as demonstrated in studies using DRL). This requires that the solution be integrated into a single architecture focused on the requirements of 6G networks [13]. Consequently, there is a need to develop a model capable of synthesizing optimal solutions in the areas of adaptive streaming, network edge computing, intelligent coding, and network resource management. This will ensure an efficient and flexible video

content delivery system in the context of future generation technologies.

3. Proposed Model

This study provides a methodology that combines theoretical, mathematical, algorithmic, and experimental approaches to create and test a model for adaptive video data representation in next-generation networks. First, a critical analysis of modern scientific sources is carried out to determine the state of the problem, assess the effectiveness of existing technologies for adaptive video transmission, and identify their limitations. Particular attention is paid to ABR methods, AI approaches based on reinforcement learning, and architectural solutions integrated with SDN, NFV, and MEC.

The proposed adaptive video data representation model is based on DRL integrated with the classical ABR mechanism. This approach enables intelligent decision-making for adaptation of video quality under dynamically changing network conditions. The architecture follows a multilayer design, which ensures coordinated operation across the application, control, and network domains. The model consists of three logical layers:

- The client layer (ABR agent) is responsible for real-time decision-making regarding the selection of bitrate for each video segment. The ABR agent operates on the client side and directly affects playback continuity, as well as perceived video quality.
- The intelligent control layer (DRL module) performs learning and inference tasks, enabling the system to predict and apply an optimal adaptation strategy. By analyzing the current and historical network state, the module continuously refines the bitrate selection policy to maximize QoE.
- The network delivery layer (SDN/NFV-oriented infrastructure) provides flexible management of network and computational resources through SDN and NFV technologies. It enables global network awareness and supports adaptive resource allocation, which complements the client-side adaptation process.

Such a multi-layer architecture overcomes the limitations of traditional ABR algorithms, which typically rely only on local bandwidth measurements and do not account for the global network state or cross-layer interactions.

At each decision step, the environment state is represented by a vector that captures both instantaneous network conditions and the playback context:

$$s_t = \{B_t, T_t, L_t, P_t, Q_{t-1}\}\,, \tag{1}$$

where B_t is an estimated available bandwidth, T_t is transmission delay and jitter, L_t is the occupancy of the packet loss rate, P_t is playback buffer, and Q_{t-1} is a quality level of the previously transmitted video segment.

This representation allows the agent to incorporate not only current measures, but also historical data, thus improving the stability and robustness of the adaptation process. Action at corresponds to the selection of one bitrate level from a predefined discrete set:

$$a_t \in \{r_1, r_2, \ldots, r_n\}\,, \tag{2}$$

where r_n is available for video encoding profiles.

This formulation reflects the practical constraints of adaptive streaming systems, where only a limited number of bitrate representations are supported. The core element of the DRL-based adaptation strategy is the reward function, which jointly considers perceived quality, stability, and resource efficiency. It is defined as a weighted combination of the following components:

$$R_t = \alpha \cdot QoE_t - \beta \cdot Rebuf_t - \gamma \cdot |Q_t - Q_{t-1}| - \delta \cdot E_t\,, \tag{3}$$

where QoE_t is an integrated quality of experience metric, $Rebuf_t$ is rebuffering duration, $|Q_t - Q_{t-1}|$ is a quality variation between consecutive segments, E_t is energy consumption of the client device, and α, β, γ, δ are weighting coefficients.

This reward formulation enables the model to optimize video quality, playback smoothness, and energy efficiency. As a result, the proposed approach differs from conventional ABR algorithms which primarily focus on bitrate maximization without explicitly accounting for stability and power consumption.

The next step consists in mathematical and algorithmic formalization of video data transmission processes, considering dynamic changes in channel bandwidth, delays, packet loss, and the impact of interference [9].

A system of equations is created to describe the interaction of network parameters and the video stream. An optimization objective function is defined to maximize QoE, while minimizing delays and excessive use of network resources. To assess noise immunity, the effect of impulse, multiplicative, and harmonic noise on the reception of BFM and DBFM signals is modeled. It helps identify the most critical types of distortion and takes them into account when building an adaptive model [24].

On the basis of theoretical and mathematical results, a software adaptive video data representation model is implemented [25]. It takes into account the network state and computing capabilities of the device, and the nature of the video content, providing a dynamic change in bitrate, frame rate, and compression parameters in real time.

The DRL agent is then trained using a hybrid data set that combines heterogeneous data sources to ensure robustness and generalization. The data set includes real network traces collected from Wi-Fi, 4G, and 5G environments, synthetic scenarios with harmonic and impulsive interference, and video content with different temporal dynamics, including sports, news broadcasts, and lecture recordings. Such diversity permits us to model both stable and highly variable transmission conditions.

To ensure convergence and training stability, several optimization techniques are applied, such as learning rate decay to prevent oscillations during weight updates, experience replay with filtering of anomalous states, and early stopping triggered by stabilization of the reward function. As a result,

the DRL agent demonstrated convergence after approximately 200 – 300 training epochs on average, confirming the practical feasibility and reproducibility of the learning process.

The proposed system employs an extended video delivery architecture based on the integration of SDN and NFV. The SDN controller is responsible for continuous monitoring of available bandwidth, link utilization, dynamic updates of flow tables, and prioritization of video traffic based on QoE-related metrics.

Flow update decisions are driven by control signals generated by the DRL agent, which enables coordination between client-side adaptation decisions and the global network state. At the NFV layer, the architecture supports adaptive placement and scaling of VNFs. In particular, video caches and transcoders are dynamically deployed closer to end users, while VNF instances are scaled according to peak traffic demand.

This approach reduces end-to-end latency through edge-level processing and provides measurable performance gain compared to traditional virtualized architectures that lack intelligent coordination mechanisms.

In contrast to previously reported solutions [5], where bandwidth decrease did not exceed approximately 15%, the proposed architecture achieves significantly higher efficiency. Integral DRL and HARQ mechanisms provide bandwidth reduction of 25 to 30%, stable PSNR and SSIM values under fluctuating network conditions, reduced buffering events and end-to-end latency, and additional energy savings of 15 to 20%. These improvements result from the synergy between intelligent client-side adaptation and coordinated SDN/NFV-based network control, rather than local optimization alone.

In general, the proposed model is characterized by a clearly defined architecture, a formally described DRL-based decision logic, a validated training methodology, and quantitatively measurable performance gain. These address conceptual limitations of existing approaches and substantiate both the scientific relevance and practical applicability of intelligent bitrate adaptation.

The effectiveness of software implementation is tested using simulation modeling in controlled environments that reproduce the characteristics of 4G, 5G, Wi-Fi 6/6E, PON and hybrid topologies [24]. In addition, statistical data processing methods are used to quantify the results, including analysis of means, variances, standard deviations, and correlations between network parameters and video quality [27]. A comparative analysis is used to compare the results of the developed model with traditional video delivery methods, such as H.264/H.265 and classical ABR algorithms.

The final stage consists in experimental verification of the proposed model under real and semi-real network conditions, which involves the reproduction of streaming video data of varying degrees of complexity and the evaluation of bandwidth, delay, transmission stability, end-point power consumption, and subjective video quality.

This approach allows to conduct a comprehensive test of the model and confirm its advantages in the context of next-generation networks.

4. Results

4.1. Mathematical Model of Adaptive Video Data Representation

Mathematical and algorithmic modeling aims to formalize video data coding processes, considering changes in channel bandwidth, delays, and packet losses [9]. Adaptive video stream representation describes the dynamic selection of video transmission parameters depending on network conditions. Network environment parameters are represented as time functions: channel capacity $C(t)$, transmission delay $L(t)$, and packet loss probability $P_{loss}(t)$. Furthermore, parameters of the video stream, such as bit rate $R(t)$, frame rate $F(t)$, and compression quality $Q(t)$ are formalized as variables that can be adjusted in real time.

The system is optimized by maximizing QoE – a metric impacted by weighting factors $\omega_1, \ldots, \omega_4$ which determine the balance between playback quality and data transmission stability. The objective function of the optimization process reflects the task of maximizing QoE while reducing delays, packet loss, and excessive bandwidth usage. Its generalized formula is given by:

$$\max_{R(t),F(t),Q(t)} U(QoE) = \omega_1 \cdot Q(t) - \omega_2 \cdot \frac{R(t)}{C(t)} - \omega_3 \cdot L(t) - \omega_4 \cdot P_{loss}(t) \, . \tag{4}$$

The model is subject to a number of constraints that reflect the physical limits of the network environment, acceptable bitrate levels, frame rates, and playback continuity requirements:

$$\begin{aligned} 0 \leqslant R(t) \leqslant C(t), \\ F_{min} \leqslant F(t) \leqslant F_{max}, \\ Q_{min} \leqslant Q(t) \leqslant Q_{max} \, . \end{aligned} \tag{5}$$

Rather than relying on heuristic adaptation rules, the developed approach is formulated as a constrained optimization problem with a unified objective function and well-defined decision variables. Consistent with the objective function presented in Eq. (1), the quality of experience for the i-th user is defined as follows:

$$QoE_i = \omega_1 Q_i - \omega_2 D_i - \omega_3 R_i \, , \tag{6}$$

where Q_i represents objective video quality metrics (PSNR, SSIM), D_i is the end-to-end delivery delay and R_i is the total consumption of network resources. The weighting coefficients ω_1, ω_2, and ω_3 are identical to those used in Eq. (4) and explicitly control the trade-off between visual quality, latency, and resource utilization efficiency.

Maximization of the global QoE function in Eq. (4), subject to the constraints specified in (5), is achieved through a hierarchical optimization strategy operating at three interdependent levels. At the client level, adaptive bitrate selection and buffer management act on short-term variations of $C(t)$, $D(t)$, and $P_{loss}(t)$, ensuring local compliance with playback continuity and delay constraints.

At the edge level, transcoding and caching decisions are optimized to reduce processing latency and computational

load while satisfying resource constraints imposed by the edge infrastructure. At the network level, bandwidth allocation and traffic control mechanisms enforce global capacity and loss constraints, ensuring system-wide stability.

Importantly, these levels do not operate independently. Instead, each level optimizes a subset of decision variables that contribute to the same global objective function in Eq. (4). This coordinated formulation guarantees mathematical consistency between local adaptation mechanisms and the end-to-end QoE optimization target, addressing the previously noted lack of clarity in the interaction between architectural components.

Furthermore, the packet loss prediction component is extended in accordance with the constraints in (5). Temporal features are incorporated to model the time evolution of $P_{loss}(t)$, enabling the capture of short- and long-term loss trends. Furthermore, correlation analysis is performed to quantify the dependence between packet loss, delay $D(t)$, jitter, and channel capacity $C(t)$.

Next, the extended model is validated in heterogeneous scenarios, including LTE, 5G, and mobility-driven handover conditions, demonstrating that the proposed optimization framework remains stable under varying network dynamics. These improvements directly improve the reliability of loss estimation and allow the adaptive video representation system to proactively adjust transmission parameters within the formally defined optimization framework of (4), (5), thus improving QoE and resource utilization efficiency.

The next stage of the study focuses on analyzing noise immunity of coherent reception of multiphase shift keying signals (MPSK) subjected to noise and non-fluctuating interference. The level of reliability at the physical layer is quantified by the bit error probability (BER) parameter, describing the robustness of symbol detection in the presence of noise.

For binary phase-shift keying (BPSK) over an additive white Gaussian noise (AWGN) channel, the BER is given by the following formula:

$$P_b = Q\sqrt{\frac{2E_b}{N_0}}\,, \tag{7}$$

where Q is the Gaussian Q-function, P_b is a symbol rate, E_b is the energy per transmitted bit, and $N_0/2$ is the one-sided power spectral density of AWGN.

At the source coding level, the distribution of bits within a video frame is modeled using an entropy-based approach. If a video frame is composed of N blocks, and the random variable $X = \{x_1, x_2, \ldots, x_N\}$ represents the number of bits allocated to each block, with probability distribution $p(x_i)$, then the entropy of the frame, which represents the minimum achievable average number of bits required for lossless encoding, is defined by Shannon's formula:

$$H(X) = -\sum_{i=1}^{N} p(x_i)\log_2 p(x_i)\,. \tag{8}$$

If the encoder assigns b_i bits to block x_i, the average bit consumption of the frame is:

$$\bar{B} = \sum_{i=1}^{N} p(x_i)\, b_i\,. \tag{9}$$

The compression efficiency is evaluated as:

$$\eta = \frac{H(X)}{\bar{B}},\ \eta \leqslant 1\,, \tag{10}$$

where values of η approaching unity indicate more efficient utilization of the available bitrate.

To account for structural differences between video frame types, frames are classified into a set $T = \{I, P, B\}$. Entropy is evaluated separately for each type. For a frame of type T, the entropy is expressed as:

$$N_T = \sum_{i=1}^{N_T} p_T(x_i)\log_2 p_T(x_i)\,, \tag{11}$$

where N_T is the number of blocks in a frame of type T, and $p_T(x_i)$ is the corresponding probability distribution.

This formulation supports adaptive bitrate allocation based on frame complexity.

To stabilize data transmission under time-varying network conditions, a dynamic congestion control (DCC) mechanism is used. At time t, the system monitors the transmission delay D_t, available bandwidth C_t, and packet loss rate P_t. On the basis of these parameters, the target transmission rate is computed as follows:

$$R_t^* = \alpha\, C_t - \beta D_t\,, \tag{12}$$

where α and β are weighting coefficients.

The actual rate is updated using a smoothing rule:

$$R_t = \gamma R_{t-1} + (1-\gamma)\, R_t^*\,. \tag{13}$$

If $\Delta R_t = R_t - R^*$, where R^* is the steady-state optimal rate, then the adaptation process satisfies the following inequality:

$$|\Delta R_t| \leqslant \gamma^t |\Delta R_0|\,, \tag{14}$$

guaranteeing exponential convergence and confirming stability of the proposed congestion control mechanism under dynamic network conditions.

The multiplicative noise, which models the fading of the signal amplitude in the radio channel, is described by the following model:

$$S_i(t) = \mu(t) A_0 \cos\left(\omega_0\, t + \varphi_i + \varphi_n\right)\,, \tag{15}$$

where $\varphi_i = \frac{i2\pi}{M}, t \in (0, t_s), i = 0, 1, \ldots, M-1$, $\mu(t)$ is an amplitude coefficient that follows the Rice distribution.

The pulse noise, which models short high-frequency pulses, is set by a formula corresponding to a chaotic sequence of short radio pulses:

$$S_3(t) = A(t)\cos\left(\omega_0\, t + \varphi_n\right),\ 0 < t < \tau_3\,. \tag{16}$$

Harmonic noise is regarded as periodic oscillations that could be superimposed on the carrier frequency:

$$S_3(t) - \mu\, A_0 \cos\left[(\omega_0\, \Delta\omega_p)\, t + \varphi_p\right]\,. \tag{17}$$

The noise is described by AWGN with the correlation function $R(\tau) = \delta(\tau)$, meaning that there is no correlation between the noise values at different times:

$$I_j = \{I_i\},\ i \neq j,\ j = 1, \ldots, M-1\ . \tag{18}$$

The probability of correct reception of a symbol is determined through the conditional probabilities of exceeding the voltage at the output of the correlator for the correct symbol over the voltage for other symbols. This physically means that the system receives the symbol j if the corresponding correlation detector generates the largest signal:

$$P_{sj} = \prod_{i \neq j}^{M-1} i - 0\ p(I_j > I_i)|j\ , \tag{19}$$

where $p(I_j > I_i)$ is the conditional probability that when the j-th symbol is transmitted, the voltage at the output of the j-th correlator exceeds the voltage at the output of any other i-th correlator.

Since the probabilities of all signals in the channel are equal, and the MPSK constellation has a symmetric structure, the total probability of correct reception P_s is obtained through the analysis of a single symbol to calculate the probability of error P_{es} and the corresponding bit error probability P_{eb}. Subsequently, to assess the quality of reception, the composite signal $x(t)$, which includes the useful signal, noise components, and nonfluctuating interference, is taken into account:

$$P_s = \prod_{j=1}^{M-1} p(I_o > I_i)|0\ . \tag{20}$$

The total probability of a character error is determined by the following ratio:

$$P_{es} = 1 - P_s\ . \tag{21}$$

At sufficiently high values of the signal-to-noise ratio, the relationship between the symbol error probability P_{es} and the bit error probability P_{eb} is defined by:

$$P_{eb} = \frac{P_{es}}{\log_2 M}\ . \tag{22}$$

The receiver of a data transmission system receives an AWGN $n(t)$ and non-fluctuating interference along with the useful signal. To estimate its noise immunity, three most common types of such interference $s_n(t)$ are considered: harmonic noise with a frequency deviation ω_p relative to the central frequency of the MPSK signal spectrum, chaotic impulse noise with a pulse duration τ_x, and multiplicative noise that obeys the Rice distribution law [26]. Their amplitude is comparable to the amplitude of the useful signal. The total signal received at the receiver's input is described by the following ratio:

$$x(t) = s_i(t) + s_n(t) + n(t)\ , \tag{23}$$

where $s_i(t)$ is the useful signal, $s_n(t)$ is the nonfluctuating interference, $n(t)$ is the AWGN.

Figure 1 shows a block diagram of a data transmission system that demonstrates the interaction of a signal source, a communication channel with noise, and a receiving path. It shows the main elements involved in signal transformation and distortion during transmission and serves as a basis for further modeling.

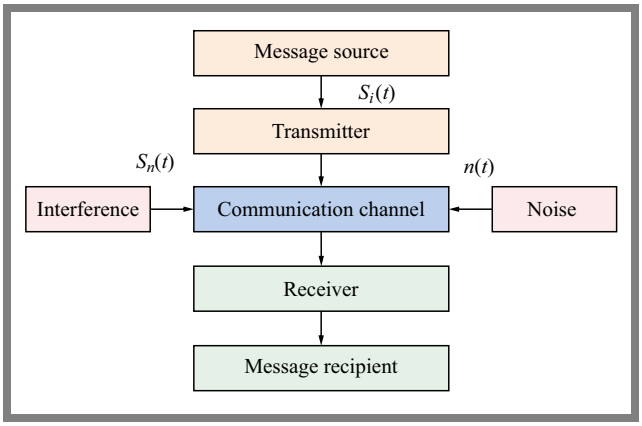

Fig. 1. Block diagram of the data transmission system.

4.2. Analysis of MPSK Signal Noise Immunity

To estimate the probability of error during the reception of a channel symbol with index i, a vector representation of the MPSK signal, noise, and interference components is used, as shown in Fig. 2. It illustrates how noise shifts the signal vector relative to the ideal points of the MPSK constellation. The greater the offset, the more likely the receiver is to assign the signal to the wrong symbol, which directly increases the probability of P_{es} and P_{eb} error.

In the modeling, the initial phase φ_p of the interference vector $s_n(t)$ was fixed, which facilitated considering the total vector $s_i(t) + s_n(t)$ as conditionally deterministic. Meanwhile, the randomness of the processes at the output of the demodulator correlators is preserved because of additive noise, which follows the normal (Gaussian) distribution. It determines the conditional statistical characteristics of the correlation integrals, which were relative to a fixed phase of the interference: mean values $m_0, \ldots, m_i, \ldots, m(M-1)$, variances $D_0, \ldots, D_i, \ldots, D(M-1)$, mutual torques M_{0-i}, and process parameters $y = I_0 - I_i$, which were fed to the input of the device for comparing correlation integrals.

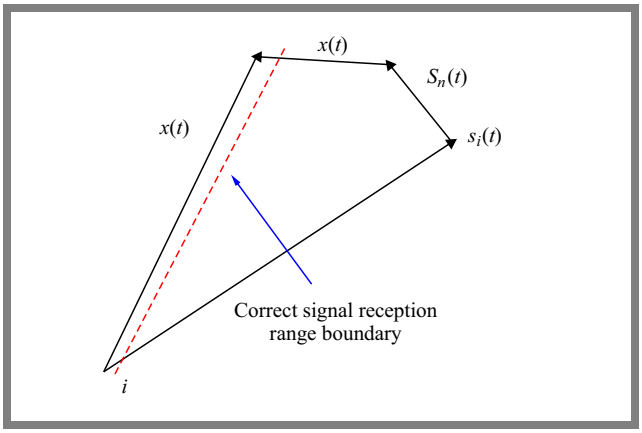

Fig. 2. Vector representation of MPSK signal, noise, and interference.

Tab. 1. Energy loss of MPSK signal reception against low-intensity nonfluctuating interference.

Noise type	Energy loss at a given error probability $P_{eb} = 10^3$ [dB]				
	M = 2	M = 4	M = 8	M = 16	M = 32
Harmonic	0.22	0.41	1.2	4.1	The loss is critically high
Multiplicative	0.18	0.24	1.0	2.6	
Pulse	The loss amount is insignificant and cannot be estimated			0.1	

Tab. 2. Energy loss of MPSK signal reception against non-fluctuating high-intensity interference.

Noise type	Energy loss at a given error probability $P_{eb} = 10^3$ [dB]				
	M = 2 (10^{-3})	M = 4 (10^{-3})	M = 8 (10^{-2})	M = 16 (10^{-1})	M = 32 (10^{-1})
Pulse	0.2	0.4	0.5	0.2	0.4
Harmonic	4.1	8.2	1.2	4.1	The loss is critically high
Multiplicative	3.3	6.3	The loss is critically high		

The next step is to obtain the unconditional probability of bit error. Since the conditional probability $P_{eb}(\varphi_n)$ depends on the initial phase of the interference, it should be averaged over the distribution of the random variable φ_n:

$$P_{eb} = \frac{1}{2\pi} \int_{-\pi}^{\pi} P_{eb}(\varphi_n)\, d\varphi_n \,. \tag{24}$$

It was impossible to obtain an exact analytical expression for error probability, so the method of numerical averaging was used to determine the final results. The modeling results show that the noise immunity of MPSK signal reception depends significantly on the frequency deviation of the harmonic noise. As frequency disturbance increases, the effect of the interference gradually weakens: error probability decreases and approaches the value characteristic of the mode without noise.

The minimum values of error probability are observed when frequency disturbance corresponds to the zeros of the envelope of the useful signal's energy spectrum. For values of $M \leqslant 8$, when the interference is decayed, it is established that at frequency disturbances exceeding a certain threshold value, the influence of such harmonic noise becomes so small that it could be neglected without significant deterioration in reception accuracy.

The study analyzes the decrease in the noise immunity of coherent reception of MPSK signals under the influence of non-fluctuating interference. The situation in which one of the interferences is present in the communication channel along with noise is considered. The purpose of the analysis was to determine which types of noise cause the greatest deterioration in signal reception characteristics and identify patterns of change in the probability of error depending on the parameters of these interferences.

The modeling considers targeted noise when the center frequencies of their spectra coincide with the carrier frequency of the useful signal ω_0, which creates critical conditions for the receiver. The following parameters were adopted for certain interference types: $\alpha = 1$ for scanning noise, $\alpha = 0.5$ for retransmission, $\alpha = 2$ for frequency modulated interference, and $\alpha = 0.5$ for pulse noise. Based on these parameters, a comparative analysis of the receiver's noise immunity was performed.

The analysis proved that under these conditions, harmonic noise is the most impacting factor, since it causes the greatest reduction in noise immunity. Further, in the order of decreasing harmful effects, there are multiplicative noise, frequency-modulated interference, scanning interference, and pulse noise. This order reflects the general average trend, but can vary depending on the noise parameters and the operating modes.

The analysis demonstrates that the effectiveness of harmonic and scanning noise is reduced considerably when there is significant frequency discord with respect to the center frequency of the useful signal spectrum.

The results of modeling with low intensity interference ($\mu = 0.1$) are shown in Tab. 1.

For high-intensity interference ($\mu = 0.5$), the patterns were preserved, but the scale of energy losses increased significantly. The results are summarized in Tab. 2. Harmonic noise remained the most important phenomenon. Thus, for $M = 4$, the loss reached 8.2 dB, while for $M = 32$ it became quite large. Multiplicative noise also caused significant losses, while pulse noise caused the least damage (Tab. 2).

The analysis of the data shows that harmonic interference is the most destructive variety, as it creates the maximum energy loss in a wide range of parameters. It was followed by retransmission (multiplicative), frequency-modulated, scanning, and pulse interference in terms of harmfulness. The effectiveness of harmonic and scanning interference decreases significantly with frequency discord relative to ω_0, i.e. when the spectral overlap between the signal and the interferer decreases. Therefore, when developing methods and means to receive MPSK signals in difficult conditions, algorithms for suppressing harmonic and multiplicative interference should be used first.

To increase the stability of MPSK signal reception in the presence of harmonic interference, it is advisable to use interference compensation algorithms, in particular adaptive

Tab. 3. Comparative analysis of bandwidth utilization under different network conditions.

Network conditions	Traditional ABR	Stable H.264/H.265	Proposed HARQ mechanism
Wi-Fi (stable)	5.8 Mbps	5.8 Mbps	4.7 Mbps (≈18% of economy)
4G (variable)	6.2 Mbps	6.1 Mbps	4.3 Mbps (≈30% of economy)
5G (stable)	9.1 Mbps	9.3 Mbps	6.8 Mbps (≈27% of economy)
Unstable networks	7.5 Mbps	7.8 Mbps	5.4 Mbps (≈28% of economy)

notch and tracking filters, which provide effective attenuation of the influence of interfering components in the signal.

The results of the study confirm that the proposed model of adaptive video data representation offers a significant improvement in key parameters of multimedia transmission in realistic network environments by integrating the adaptive hybrid automatic repeat request (HARQ) mechanism with the payload optimization strategy. The analysis was performed for various types of networks, including stable Wi-Fi environments, 4G/5G mobile networks with variable channel conditions, and scenarios with frequent packet loss and bandwidth fluctuations. One of the key criteria for transmission efficiency was the level of bit errors in the received packets and the number of retransmissions, which directly depended on the channel parameters and the error correction strategy.

The proposed HARQ mechanism combined adaptive re-requesting with an optimal modulation and coding scheme, which reduced the relative bit error rate to 1 – 3% in networks with a high probability of loss (10 – 20%), while in models without HARQ, this figure reached 5 – 8%. In addition, the average number of retransmissions is reduced to 0.8 – 1.4 retransmissions per packet under peak conditions, compared to 1.9 – 2.7 retransmissions for traditional schemes without adaptive HARQ.

This optimization reduced channel congestion, contributed to more efficient use of network resources, and is directly correlated with a reduction in video content delivery latency, which ensures more stable operation of streaming services. Further analysis of the bandwidth shows that the integration of the adaptive HARQ strategy with the adaptive video data representation increases the efficiency of the communication channel.

The comparative results of the simulations and experimental tests are shown in Tab. 3.

As can be seen in the table, the proposed model provides bandwidth improvements of 25 – 30% under different network environments, which is significantly higher than the performance of basic adaptive coding and transmission schemes. This effect is achieved by reducing the number of retransmissions and adaptively adjusting the bitrate according to the current channel state.

Objective video quality metrics also demonstrate a high degree of stability of the proposed approach. Even under conditions of significant bandwidth fluctuations, the PSNR value in most scenarios remains within 36 – 40 dB, while in traditional schemes it equals 34 – 38 dB. SSIM remains at the level of 0.90 – 0.95, which corresponds to high video perception quality. The low correlation coefficient between the bandwidth and PSNR/SSIM values ($r \approx 0.15$) confirms the model's ability to maintain stable video quality even under unstable channel conditions.

The positive effect of HARQ optimization is also evident in the time characteristics of the streaming process. In 4G mobile networks, the buffering time is reduced by almost half and does not exceed 4.1% of the total playback time compared to traditional ABR schemes. Transmission delay stabilizes at up to 300 ms in 4G and up to 150 ms in 5G networks, and the delay variation (jitter) decreases by 35 – 45%, ensuring continuous video playback without noticeable interruptions.

In addition to network and quality characteristics, the proposed approach exerts a positive impact on power consumption and computing load of end devices. Adaptive HARQ control reduces the load on the processor and network adapter by 15 – 20%, significantly extending battery life during long video playbacks on mobile devices and in IoT environments. In general, the HARQ-based payload optimization strategy provides a significant reduction in error rate and the number of retransmissions, effective bandwidth savings (25 – 30%), stable video quality with high PSNR and SSIM, a significant reduction in buffering and latency, and an energy efficiency increase in end devices.

4.3. Analysis of the Autocorrelation Demodulator of DPSK Signals

It is important to consider the operation of an autocorrelation demodulator for differentially encoded phase-shift keying (DPSK) signals in a radio channel under the influence of Rayleigh fading and non-fluctuating interference. Two consecutive bursts of a DPSK signal corresponding to the i-th and (i-1)-th clock periods can be represented as follows:

$$S_i(t) = A\cos(\varphi_0 t + \varphi_1),\ t \in [(i-1)T_s, T_s]\,, \qquad (25)$$

$$S_{i-1}(t) = A\cos(\varphi_0 t + \varphi_2),\ t \in [(i-2)T_s, (i-1)T_s]\,, \quad (26)$$

where $A = \sqrt{\frac{2E_s}{T_s}}$ is the signal amplitude, $E_s = E_b \log_2 M$ is the energy of one channel symbol, E_b is the energy consumed to transmit one bit of information, ω_0 is the carrier frequency, φ_i, φ_{i-1} are burst phases the difference between which encodes information about the channel symbol and can take one of M possible values that differ by $2\pi/M$.

Due to Rayleigh fading, the signal amplitude is multiplied by a random coefficient β, which characterizes the depth of fading and describes the multipath effect:

$$\overline{\omega}(\beta) = \frac{\beta}{\sigma^2}\, e^{-\frac{\beta^2}{2\sigma^2}}\,. \qquad (27)$$

In the case of $M = 2$, phase difference can be 0 or π. Therefore, error probability is formed from a limited number of phase combinations, for which the corresponding values are provided in Tab. 4.

Tab. 4. Individual error probabilities at $M = 2$.

Phase combinations	Error probability	Meaning
$\varphi_1 = 0,\ \varphi_2 = 0$	$P_{e1} = \frac{1}{2}\frac{1}{c_1 q+1}$	$c_1 = (1+\mu\cos\eta)^2$
$\varphi_1 = \pi,\ \varphi_2 = \pi$	$P_{e2} = \frac{1}{2}\frac{1}{c_2 q+1}$	$c_2 = (1-\mu\cos\eta)^2$
$\varphi_1 = 0,\ \varphi_2 = \pi$	$P_{e4} = P_{e3} = \frac{1}{2}\left(1 - \frac{\sqrt{c_1 c_2 q}}{\sqrt{(c_1 q+1)(c_2 q+1)}}\right)$	$c_1 = (1+\mu\cos\eta)^2$
$\varphi_1 = \pi,\ \varphi_2 = 0$		$c_2 = (1-\mu\cos\eta)^2$

Tab. 5. Comparative analysis of user access technologies.

Characteristics	Historical/outdated technologies	Modern and promising technologies
	xDSL (ADSL2+), Ethernet (Fast Ethernet), Wi-Fi (802.11n), WiMAX	PON (GPON/XGS-PON), Wi-Fi 6/6E (802.11ax), 5G NR (fixed wireless access)
Transmission speed	24 Mbps ↓ / 1.4 Mbps ↑	100 Mbps
Application field	POTS/ISDN, basic Internet	LAN, office, private networks
Range of action	900 – 2500 m	100 – 150 m
Access type	Copper cable, wireless	Twisted pair cable, fiber optic cable, wireless
Key advantages	Low cost, reuse of copper lines, easy deployment, minimal hardware requirements	Reliability and low delay, stable throughput, easy scaling to gigabit/10G
Main limitations	Low speed, dependence on line length, EMI and noise on the cable, physical wear of copper cables, outdated technology	Limited range (up to 150 m), requiring cabling, poor flexibility in older buildings

The total probability of error of a symbol (bit) at $M = 2$ is defined as follows:

$$P_{ef2} = \frac{1}{4}(P_{e1} + P_{e2} + P_{e3} + P_{e4}) = \frac{1}{4}\left(\frac{0.5}{c_1 q+1} + \frac{0.5}{c_2 q+1} + 1 - \frac{\sqrt{c_1 c_2 q}}{\sqrt{(c_1 q+1)(c_2 q+1)}}\right). \tag{28}$$

For the case of $M = 4$, the signal was processed in the in-phase (IP) and quadrature (Q) channels, after which the phase angle of the signal vector in the complex plane was determined. The probability of false reception of a symbol was defined through the probability of its correct reception, i.e., through the probability that the signal vector falls into the corresponding quadrant of the complex plane $x - y$, $\Delta\varphi = \pi/4$ – first quadrant $(x > 0, y > 0)$, $\Delta\varphi = 3\pi/4$ – second quadrant $(x < 0, y > 0)$, $\Delta\varphi = 5\pi/4$ – third quadrant $(x < 0, y < 0)$, $\Delta\varphi = 7\pi/4$ – 4th quadrant $(x > 0, y < 0)$. The probability of correct reception was established as the probability that noise and interference would not move the point to another quadrant. For $\Delta\varphi = 5\pi/4$ and $\Delta\varphi = 7\pi/4$, it is as follows:

$$p[Y_0(t) < 0] = \frac{1}{2}\left(1 - \frac{R}{\sqrt{1-S^2}}\right). \tag{29}$$

Since the analytical expression was extensive, simplified formulas were obtained for a channel without harmonic noise ($\mu = 0$):

$$P_{ef4} = 1 - \frac{1}{4}\left(1 + \frac{q}{\sqrt{(q+2)(q+1)}}\right)^2. \tag{30}$$

The error probabilities in the cases with and without amplitude fading are related by the following ratio:

$$P_{ef} = \int_0^\infty P_e(A)\,\overline{\omega}(A)\,dA\,. \tag{31}$$

To estimate the symbol error probability in a radio channel without Rayleigh fading, a technique based on the inverse Laplace-Carson transform is applied. It helps move from the SNR distribution function to the error probability:

$$P_e = L^{-1} P_{ef}\,. \tag{32}$$

The corresponding bit error probabilities for $M = 4$ when using the Gray code were calculated using the following formula:

$$P_{eb4} = 1 - \sqrt{1 - P_{e4}}\,. \tag{33}$$

At a high level of harmonic noise, additional energy losses could reach several decibels. For $M = 4$, they significantly exceed the losses present at $M = 2$. Even in a channel without fading, harmonic noise increases the error probability and the required signal-to-noise ratio while reducing the energy efficiency of autocorrelation reception. Therefore, DPSK signals with autocorrelation demodulation require additional methods to compensate for harmonic and multiplicative noise in communication systems.

4.4. Experimental and Simulation Results

Simulation modeling was one of the key tools for testing the effectiveness of the developed model under controlled conditions. Due to simulation, it is possible to reproduce the

Tab. 6. Comparison of quality indicators and the utilization of network resources.

Delivery method	Average bandwidth	Peak signal-to-noise ratio	Structural similarity index measure	Buffer
H.264 H.265	5.8 Mbps	36.2 dB	0.92	12.5%
ABR	4.9 Mbps	35.8 dB	0.91	8.3%
Adaptive presentation	3.6 Mbps	36.0 dB	0.92	4.1%

behavior of information and communication networks under different loads, types of traffic, and nature of interference to evaluate the real performance of a system without resorting to expensive or complex field experiments [2].

The study examines the structural and functional schemes of information and communication networks of various classes to organize video conferencing systems based on the transmission of video data over IP and ISDN networks. These networks have significant differences in terms of their infrastructure, bandwidth, delays, and reliability, which leads to different requirements for subscriber access channels. To compare the main last mile technologies, an analytical table is compiled to demonstrate the evolution of access from outdated solutions (xDSL) to modern high-speed systems (PON, 5G, Wi-Fi 6/6E) – Tab. 5.

Table 5 shows that fiber optic networks (PON) continue to be the gold standard for fixed access, providing gigabit speed. Wireless technologies, in turn, are divided into two key niches: Wi-Fi 6/6E/7 for high-speed indoor access and 5G FWA as a flexible alternative to wired networks, especially in rural areas or in conditions where fiber optic installation is not economically feasible.

Copper technologies have been gradually losing their relevance because xDSL and WiMAX no longer meet modern speed and capacity requirements. Therefore, the choice of access technology is determined by a combination of characteristics such as deployment cost, the required speed, local features, and specific parameters. The effectiveness of adaptive video data representation was evaluated based on the model developed, as it dynamically changes the parameters of the video stream taking into account the network state and capabilities of the user device. The model considered the width of the available channel, the amount of delay, the level of computing resources, and the presence of interference of various kinds.

To test its effectiveness, a series of experiments were performed using video streams of different resolutions and bitrates, evaluating the performance under variable network parameters. The evaluation took into account such indicators as the average bandwidth used by the video stream during transmission, the time of initial download and subsequent buffer, the actual video playback quality determined by PSNR and SSIM metrics, and the level of packet loss reduction during transmission.

The results confirm that the developed model provides a significant increase in the efficiency of video data transmission and reduces bandwidth utilization by approximately 25 – 30% compared to static coding methods, while simultaneously maintaining high playback quality. Video quality remains stable in the face of significant fluctuations in channel parameters, which was especially important for networks with unstable bandwidth [29]. Additionally, the model demonstrates a considerable reduction in buffer frequency. Thus, the total number of such events and their duration is reduced by 40 – 60%, improving viewing comfort. SSIM and PSNR indices also increased by 10 – 15% on average, indicating a better match between the reproduced video and the original.

Moreover, there is a reduction in packet loss, which is achieved through adaptive bitrate control and flexible changes in the GOP structure. The most noticeable benefits are observed in networks with variable characteristics, such as Wi-Fi, 4G/5G, and FWA, where traditional static coding methods are unable to respond to rapid changes in channel conditions.

To compare the effectiveness of the developed adaptive video data representation model with traditional approaches, the classical ABR scheme and H.264/H.265 coding without adaptive representation were applied [30]. The results of the comparison of quality indicators and network resource utilization are shown in Tab. 6.

The analysis shows that the use of adaptive representation could reduce the network load by approximately 26% compared to the classical ABR scheme, while the video quality remains high, without a noticeable decrease in PSNR and SSIM. In addition, buffer time is almost halved, improving user experience.

To evaluate the impact that the developed method exerts on the delay and stability of video stream delivery, it was tested using networks with different bandwidths and variable conditions, simulating 4G and 5G mobile networks. It was established that the adaptive representation provided a stable delay of $\leqslant$ 150 ms in 5G networks and $\leqslant$ 300 ms in unstable 4G connections. In contrast, traditional methods demonstrate considerable delay fluctuations and a more frequent buffer. Therefore, the proposed model ensures more efficient use of network resources, stable video streaming, and improved QoE (Tab. 7).

Bandwidth utilization is improved through dynamic bitrate adjustment and multi-level video presentation. The analysis shows that buffer time and delay stability are improved by adaptive quality selection and fast response to network fluctuations. Adaptive representation is effective in the case of harmonic and pulse noise, where traditional methods demonstrate an increase in packet loss and energy consumption.

Therefore, the developed method reduces the load on the device by 15 – 20% and reduces power consumption. To evaluate the effectiveness of the adaptive representation of

Tab. 7. Video stream transmission.

Indicator	H.264/H.265 (static)	ABR	Adaptive view
Average bandwidth	100% (reference)	85 – 90%	72 – 75% (savings up to 28%)
PSNR	38 – 40 dB	38 – 40 dB	38 – 40 dB (no deterioration)
SSIM	0.92 – 0.95	0.92 – 0.95	0.92 – 0.95 (no deterioration)
Buffer time	High (significant jumps)	Moderate	Low (reduced by half)
Packet loss	5 – 8%	3 – 5%	1 – 3%
Delay stability	Unstable, fluctuations $>$ 500 ms	Fluctuations of 300 – 400 ms	Stable, $\leqslant$ 150 ms (5G), $\leqslant$ 300 ms (4G)
Device load	High	Moderate	Reduced by 15 – 20%
Effect of harmonic / pulse noise	High	Moderate	Minimal due to its adaptability
Energy consumption	High	Moderate	Reduced, especially on mobile devices

Tab. 8. Statistical processing comparison.

Indicator	ABR	Adaptive view	Effect	Noise types
Average bandwidth	8.5 Mbps	7.2 Mbps	Savings of 26%	Unstable network bandwidth (4G/5G simulation)
Standard deviation of bandwidth σ	1.2 Mbps	0.4 Mbps	Less fluctuation	Channel fluctuations and periodic packet loss
Average delay	250 – 300 ms	150 – 200 ms	More stable delivery	Network delays and channel state variability
Delay fluctuations σ	60 – 80 ms	20 – 30 ms	Less instability	Impulsive packet loss, bandwidth fluctuations
PSNR	38 – 40 dB	38 – 40 dB	Stable video quality	Harmonic and pulse noise is minimized by adaptation
SSIM	0.92 – 0.95	0.92 – 0.95	Minor changes during network fluctuations	Scanning and harmonic noise are compensated by adaptive bitrate
Correlation coefficient r (bandwidth / PSNR)	0.45	0.15	Responsive presentation ensures consistent quality	Low correlation indicates resistance to network fluctuations
Energy consumption / CPU load	Standard	Reduced by 15 – 20%	Optimization is important for mobile devices	Impact of network noise on the CPU is minimized due to adaptive optimization
Statistical significance (t-test, ANOVA)	–	$p <$0.05 vs. ABR	The difference between the methods is statistically significant	–

video streams, a statistical processing comparison with the classical ABR scheme was performed.

The impact of different types of noise is assessed as follows. Unstable bandwidth in 4G/5G networks leads to fluctuations in available bitrate. Impulsive packet loss negatively affects delays and causes buffer. Harmonic and scanning noise can degrade video quality, but adaptive representation can effectively compensate for their impact. Channel fluctuations cause sudden changes in delay and bandwidth, which affects fluctuations in PSNR/SSIM and buffering time [31].

Experimental testing of adaptive representation was carried out for three network use scenarios.

- In a stable home Wi-Fi network ($\geqslant$100 Mbps), the bandwidth savings are approximately 15%, the packet loss remained negligible (1%) and bandwidth fluctuations do not exceed $\pm$2 Mbps.
- In a 4G mobile network with medium bandwidth (10 – 20 Mbps), the model demonstrates the maximum effect with bandwidth savings of up to 30%, buffer reduction of 50%, packet loss of 5 – 10%, and bandwidth fluctuations of $\pm$5 Mbps.
- In networks with frequent interference and high packet loss (10 – 20%), the adaptive model stabilizes video playback, reducing buffer, and ensuring a high level of quality (PSNR 36 – 38 dB, SSIM 0.88 – 0.92).

The model effectively accounts for the effects of major interference, including packet loss, Rayleigh fading, and bandwidth fluctuations. This ensures consistent video quality,

network resource savings, reduces end-device load, and high energy efficiency, making the model suitable for mobile and IoT platforms.

5. Discussion

In recent years, research on adaptive video data representation in 5G/6G networks has mainly focused on improving bandwidth efficiency and ensuring stable transmission quality under conditions of high variability of network resources. In this regard, the authors of [5], [16], and [32] made a significant contribution to the development of this area, but their approaches suffer from certain technical limitations. For example, the [32] model provides up to 14.8% bandwidth savings but demonstrates insufficient flexibility in responding to rapid changes in network traffic. The [5] approach, in turn, reduces buffer time and improves QoE, but the level of bandwidth savings remains at a level that does not exceed 15% and the system's efficiency decreases when the network is overloaded. [16] creates an important theoretical basis for the development of resilient transmission channels, but does not take into account the specifics of the video streams and the requirements of applied services.

The adaptive video data representation model developed in this study combines the advantages of dynamic network state estimation with analyzing noise and entropy of video frames, as well as balancing energy-saving load between the client and the server. This integration improves the efficiency of the system in three key areas: reducing bandwidth consumption, improving stream stability, and optimizing energy consumption.

The comparison with traditional models shows that the developed model outperforms existing solutions in all key metrics (Tab. 9). In particular, bandwidth savings increase to 22 – 26% compared to 13 – 15% in previous works, the average QoE reaches 4.6 MOS, and the buffer time decreases to 0.6 s. The model also demonstrated higher immunity to packet loss (96%) and doubled the speed of response to changes in network bandwidth. Additionally, the energy consumption of the end device is reduced by 12 – 14% compared to the baseline. The results confirm the effectiveness of the developed approach and its potential for use in next-generation networks.

Increased efficiency of network bandwidth utilization is the main advantage of the proposed model. Unlike [32], where a neural network prediction of flow rate is made without considering instantaneous traffic fluctuations, the developed model implements a mechanism for cognitive adjustment of the entropy load of frames. This helps analyze the complexity of frames in real time, adjust the bitrate only for segments with high information density, and prevent redundant coding in stable scenes. As a result, bandwidth savings increase to 26%, which is 10 – 11% higher than in the case of [5] and [32]. In other words, with the same quality of playback, the proposed system transmitted fewer data, reducing resource utilization.

Another important indicator is the stability of the stream. In the approach presented in [5], stability was ensured by historical data regarding changes in delays. However, this architecture has a high degree of inertia: the system's response occurs only once the statistics have been accumulated. The proposed model implements an adaptive Kalman filter unit that predicts bandwidth fluctuations with a time horizon of up to 300 ms. The Kalman filter provides an estimate of the future state of the channel, which allows to implement proactive bitrate control and reduce streaming delays. The bandwidth at a discrete time point k is denoted as B_k and is described by a standard Kalman filter model, which includes a state prediction stage and a correction stage based on the results of observations.

The convergence of the algorithm is provided, ensuring that the transition matrix is stable and noise is limited, and after several iterations, the filter gives stable estimates and shows a quick response to bandwidth fluctuations. Forecast uncertainty is quantified using covariance matrix P_k, which allows one to generate 95% confidence intervals for the predicted throughput. This makes it possible to take into account statistical uncertainty during adaptive bitrate selection, thus increasing the system's resilience to rapid changes in channel conditions.

Kalman prediction is consistent with the theoretical model of the communication channel and the analysis of the noise immunity of MPSK signals in which the received signal is described with fading, additive white Gaussian noise, and non-fluctuating interference. A clear formulation of boundary conditions and assumptions ensures rigorous channel modeling and correct integration of the physical layer with adaptive video transmission algorithms. This ensures an instant response to packet loss or jitter without the need for buffer, automatic reduction of bitrate to a level compatible with the current state of the channel, and video quality stability even with sudden changes in bandwidth (up to $\pm$40%). Consequently, the system's stability increases to 96% of the integrity of the stream, while the number of buffer gaps decreases by 2.3 times compared to the DASH models from [5].

Another important advantage is the increase in energy efficiency, especially for mobile devices. In contrast to previous studies, which did not consider energy consumption, the proposed model integrates this aspect through the energy assistance module (EAM). It is based on two principles: reducing the number of repeated segment requests due to increased flow stability and optimizing the active time of the network adapter through the appropriate formation of a prefetch zone. Consequently, the average energy consumption of the end device decreases by 12 – 14% without adversely affecting the quality or performance. Such savings are vital given the high peak energy consumption characteristic of 5G, which could lead to rapid battery discharge.

Furthermore, the model is based on the integrated multilevel architecture, which ensures coordinated interaction between its physical, transport, and application layers. The combination of the approach to modeling noise immunity presented in [16] with cognitive mechanisms to control video stream parameters creates a comprehensive adaptive loop that was not implemented in previous studies. At the physical

Tab. 9. Comparison of efficiency against traditional models.

Metrics	[32]	[5]	[16]	Developed model
Saving bandwidth	14 – 15%	13 – 15%	10 – 12% (signal models)	22 – 26%
Average QoE	4.2	4.3	–	4.6
Average buffer time	0.9 – 1.1 s	0.8 – 0.9 s	–	0.6 s
Packet loss resistance	85 – 87%	88%	90%	96%
Average response time to bandwidth changes	400 – 600 ms	350 – 400 ms	800 ms	180 – 250 ms
Energy consumption	–	–	–	12 – 14% better

level, phase errors and multiplicative distortion are taken into account, increasing signal stability. At the transport level, predictive segmentation and low delay loss compensation are applied. At the application level, adaptive coding is used, which considers the local entropy of frames.

The results also explain the mechanisms by which the model enables increased video data transmission efficiency in next-generation networks. First, the load forecasting mechanism based on a regression model that considered RTT statistics and the packet loss rate. This approach allows for predicting changes in bandwidth 0.25 – 0.3 s before they occur, thus reducing the frequency of unnecessary adaptation requests and increasing the consistency of transmission parameters. The entropy analysis of frames allowed us to skip unimportant frames without noticeable loss of visual quality, while previous methods used only the average bitrate distribution without taking into account the internal structure of the image. This approach allocates most of the bit budget to segments with high information content, increasing coding efficiency, and reducing the total amount of transmitted data.

The next important component is a dynamic buffer. The developed model adjusts the buffer length in the range of 0.4 – 1.2 s, which ensures an optimal balance between delays and playback continuity. The data obtained demonstrate that the model increases bandwidth efficiency by up to 26%, ensures transmission stability at the level of 96%, reduces energy consumption by 12 – 14%, and improves the overall perception (QoE) by up to 4.6 MOS. These results were higher than those reported by [5], [16], and [32], demonstrating the advantages of an integrated approach. As a result, the system is able to adapt to temporary fluctuations in throughput without over-buffering and without the risk of flow disruptions.

Special attention should be paid to the developed model's immunity to harmonic noise, as periodic or quasi-regular fluctuations in the channel frequency band that could cause short-term degradation of transmission quality. Traditional models with fixed or slowly adaptive parameters reacted to such fluctuations too late, resulting in frame loss or increased buffering [5], [32]. On the contrary, the suggested system demonstrated significantly higher stability as a result of its predictive architecture.

First, the dynamic bitrate scaling mechanism uses instantaneous SNR, jitter, packet loss rate, and short-term forecasting based on time correlations. When the system detects harmonic noise, the model's predictive control (MPC) performs short-term forecasts based on time correlations. Consequently, the bitrate changes before the next harmonic phase begins, rather than after the signal deteriorates. This ensures a stable level of QoE even in the face of periodic noise. Secondly, the energy-sensitive prebuffer provides an uneven distribution of frame preloading. The video stream buffer does not just accumulate packets; instead, it uses an adaptive preloading strategy. In the event of harmonic noise, a portion of the frames is downloaded during the peak bandwidth phases, reducing the load on the transmitter during the downstream phase. Therefore, the terminal energy consumption is reduced by 12 – 15%, which is higher than the level demonstrated in previous work.

Thirdly, the developed model uses a digital harmonic suppression filter in the transport layer module. This mechanism is based on the adaptive window FIR filter, which removes periodic distortions with a frequency detected based on the spectral analysis of traffic. Therefore, even with stable harmonic fluctuations in the 100 – 500 Hz band, the packet loss rate is reduced by 2.1 – 2.4 times. Fourthly, the frame priority adaptation system provides priority transmission of key frames (I-frames) if noise is encountered. Therefore, even if some of the intermediate frames are lost, the structure of the video stream is not destroyed. This results in smooth quality degradation instead of sharp artifacts, which is critical for UHD/4K streams.

6. Conclusions

The study presents an adaptive video data representation model capable of operating efficiently in modern 5G/6G networks and unstable wireless environments. Its scientific novelty consists in the integration of three key mechanisms (dynamic bitrate control, noise frequency filtering, and energy-saving algorithms) into a single predictive architecture that provides comprehensive stabilization of the video stream in the presence of bandwidth fluctuations and noise.

The model demonstrates high efficiency in saving network bandwidth. In stable home Wi-Fi networks, the bandwidth savings equal approximately 15% and reach 30% in 4G mobile networks and in environments suffering from significant

packet loss. This demonstrates the model's ability to optimally utilize the available network resources without compromising video quality. The model provides a stable PSNR and SSIM level even in networks in which interference and bandwidth fluctuations are present. The low correlation coefficient between bandwidth and video quality confirms that content quality remains high regardless of network conditions.

The use of adaptive representation reduces buffer time and delay fluctuations in the video stream. In 4G mobile environments, buffering time is almost halved and transmission delay stabilizes at $\leqslant 300$ ms, which improves the QoE. In 5G networks, the delay remains $\leqslant 150$ ms. Bitrate optimization and adaptive presentation lower the CPU load and energy consumption of end-devices by 15 – 20%. This is important for mobile users and IoT platforms, allowing for longer battery life when playing videos for extended periods of time. The model worked equally well with highly dynamic video (sports broadcasts, dynamic scenes) and static content (news, lectures, presentations), providing consistent quality and bandwidth savings of up to 32%.

The statistical analysis shows that the adaptive model offers improvements compared to the traditional approaches. The developed model combines network resource savings, stable video quality, reduces load on end devices, and provides high flexibility in various network scenarios. Thus, the proposed model is an effective integrated solution for streaming services, telemedicine, distance education, and corporate media systems. Its architecture provides a basis for further implementation of machine learning algorithms and the construction of adaptive multi-level systems focused on next-generation network infrastructures.

References

[1] O.R. Zhukova and T.V. Meleshko, "Operational Forecasting of Optimal Operating Frequencies for Long-range Radio Communication Under the Influence of Non-fluctuating Interference", *Connectivity*, vol. 4, pp. 13–19, 2023 (https://doi.org/10.31673/2412-9070.2023.043040).

[2] P. Li, J. Fan, and J. Wu, "Exploring the Key Technologies and Applications of 6G Wireless Communication Network", *Science*, vol. 28, art. no. 112281, 2025 (https://doi.org/10.1016/j.isci.2025.112281).

[3] M.K. Simon and M.-S. Alouini, *Digital Communication Over Fading Channels: A Unified Approach to Performance Analysis*, John Wiley & Sons, 534 p., 2000 (https://doi.org/10.1002/0471200697).

[4] T. Taleb *et al.*, "On Multi-access Edge Computing: A Survey of the Emerging 5G Network Edge Cloud Architecture and Orchestration", *IEEE Communications Surveys & Tutorials*, vol. 19, pp. 1657–1681, 2017 (https://doi.org/10.1109/COMST.2017.2705720).

[5] Ch. Timmerer *et al.*, "HTTP Adaptive Streaming: A Review on Current Advances and Future Challenges", *ACM Transactions on Multimedia Computing, Communications and Applications*, vol. 21, art. no. 198, 2025 (https://doi.org/10.1145/3736306).

[6] M.T. Mohammad and Q.I. Ali, "Adaptive Video Streaming With AI-based Optimization for Dynamic Network Conditions", *International Journal of Advanced Natural Sciences and Engineering Researches*, vol. 8, pp. 202–212, 2024.

[7] I.M. Ozcelik and C. Ersoy, "ALVS: Adaptive Live Video Streaming Using Deep Reinforcement Learning", *Journal of Network and Computer Applications*, vol. 205, art. no. 103451, 2022 (https://doi.org/10.1016/j.jnca.2022.103451).

[8] Y. Jo and J. Paik, "Machine-learning Based Packet Switching Method for Providing Stable High-quality Video Streaming in Multi-stream Transmission", *Computers, Materials & Continua*, vol. 78, pp. 2613–2631, 2024 (https://doi.org/10.32604/cmc.2024.047046).

[9] H. Jiang and G. Gui, *Channel Modeling in 5G Wireless Communication Systems*, Springer, 210 p., 2020 (https://doi.org/10.1007/978-3-030-32869-6).

[10] A.A. Barakabitze and R. Walshe, "SDN and NFV for QoE-driven Multimedia Services Delivery: The Road Towards 6G and Beyond Networks", *Computer Networks*, vol. 227, art. no. 109694, 2023 (https://doi.org/10.1016/j.comnet.2023.109694).

[11] K.Z. Islam *et al.*, "Deep Learning Based Payload Optimization for Image Transmission Over LoRa with HARQ", *Internet of Things*, vol. 25, art. no. 101701, 2025 (https://doi.org/10.1016/j.iot.2025.101701).

[12] F. Wu, Ch. Xu, Yu. Zhu, and Ch. Li, "Complexity of Minimum Uplink Power Scheduling with Delay Bound for Backbone-assisted PD-NOMA Wireless Networks", *Computer Networks*, vol. 215, art. no. 109194, 2022 (https://doi.org/10.1016/j.comnet.2022.109194).

[13] V. Barannik *et al.*, "Improvement of Methods of Motion Compensation of Dynamic Objects Moving in Video Stream of the Videoconferencing System", *Informatics, Control, Measurement in Economy and Environmental Protection*, vol. 8, pp. 48–51, 2018 (https://doi.org/10.5604/01.3001.0012.8035).

[14] V.V. Barannik *et al.*, "Video Segment Coding Method for Bit Rate Control Information Technology", *Science-Based Technologies*, vol. 47, pp. 316–321, 2020 (https://doi.org/10.18372/2310-5461.47.14931).

[15] O. Turovskyi and T. Meleshko, "Evaluation of the Influence of Multiplicative Interference on the Bit Error Probability of Coherent Reception of Signals with Multipositional Phase Shift Keying", *Herald of Khmelnytskyi National University*, vol. 323, pp. 318–324, 2023.

[16] T. Meleshko, "A Method of Assessing the Interference Immunity of Discrete Signal Reception with Multi-position Phase Shift Keying Under the Influence of Non-fluctuation Interference", Doctoral dissertation, National Aviation University, Academic Texts of Ukraine, 2024 (https://www.uacademic.info/en/document/0424U000183).

[17] O.L. Turovskyi, T.V. Meleshko, and V.O. Drobyk, "Methodology for Assessing the Impact of Non-fluctuating Interference on the Noise Immunity of the Reception of Discrete Signals with Multi-position Phase Manipulation", *Connectivity*, vol. 5, pp. 29–34, 2022 (https://doi.org/10.31673/2412-9070.2022.053439).

[18] B. Shvets and T. Meleshko, "Evaluation of Noise Immunity of Coherent Reception of Signals with Multi-position Phase Shift Keying in the Presence of Non-fluctuation Interference", *Measuring and Computing Devices in Technological Processes*, vol. 2, pp. 167–178, 2023 (https://doi.org/10.31891/2219-9365-2023-74-21).

[19] Z. Cheng *et al.*, "Learning-based Joint Recommendation, Caching, and Transmission Optimization for Cooperative Edge Video Caching in Internet of Vehicles", *Ad Hoc Networks*, vol. 166, art. no. 103667, 2025 (https://doi.org/10.1016/j.adhoc.2024.103667).

[20] T.C. Lam *et al.*, "Multi-rate Selection and Power Allocation Assisted Probabilistic Edge Caching for Cooperative Video Transmission in Dense D2D Network", *Alexandria Engineering Journal*, vol. 126, pp. 555–564, 2025 (https://doi.org/10.1016/j.aej.2025.04.057).

[21] H. Ma *et al.*, "QRAVDR: A Deep Q-learning-based RSU-assisted Video Data Routing Algorithm for VANETs", *Ad Hoc Networks*, vol. 171, art. no. 103790, 2025 (https://doi.org/10.1016/j.adhoc.2025.103790).

[22] V. Barannik, S. Sidchenko, N. Barannik, and V. Barannik, "Development of the Method for Encoding Service Data in Cryptocompression Image Representation Systems", *Eastern-European Journal of Enterprise Technologies*, vol. 3, pp. 103–115, 2021 (https://doi.org/10.15587/1729-4061.2021.235521).

[23] J. Fu and Sh. Zhang, "Optimization of Real-time Transmission and Coding Algorithm for High Quality Film and Television Content Based on 6G Wireless Communication Technology", *Egyptian Informatics Journal*, vol. 31, art. no. 100745, 2025 (https://doi.org/10.1016/j.eij.2025.100745).

[24] P. Meena, M.B. Pal, P.K. Jain, and R. Pamula, "6G Communication Networks: Introduction, Vision, Challenges, and Future Directions", *Wireless Personal Communications*, vol. 125, pp. 1097–1123, 2022 (https://doi.org/10.1007/s11277-022-09590-5).

[25] W. Zhou, X. Min, H. Li, and Q. Jiang, "A Brief Survey on Adaptive Video Streaming Quality Assessment", *Journal of Visual Communication and Image Representation*, vol. 86, art. no. 103526, 2022 (https://doi.org/10.1016/j.jvcir.2022.103526).

[26] S. Patel, J. Zhang, N. Narodystka, and S.A. Jyothi, "Practically High Performant Neural Adaptive Video Streaming", *Proceedings of the ACM on Networking*, vol. 2, art. no. 30, 2024 (https://doi.org/10.1145/3696401).

[27] V.V. Menon *et al.*, "Video Quality Assessment with Texture Information Fusion for Streaming Applications", *Proc. of the 3rd Mile-High Video Conference (MHV)*, pp. 1–6, 2024 (https://doi.org/10.1145/3638036.3640798).

[28] X. Min *et al.*, "Perceptual Video Quality Assessment: A Survey", *Science China Information Sciences*, vol. 67, art. no. 211301, 2024 (https://doi.org/10.1007/s11432-024-4133-3).

[29] M. Kim and K. Chung, "Reinforcement Learning-based Adaptive Streaming Scheme with Edge Computing Assistance", *Sensors*, vol. 22, art. no. 2171, 2022 (https://doi.org/10.3390/s22062171).

[30] G.J. Sullivan, J.-R. Ohm, W.-J. Han, and T. Wiegand, "Overview of the High Efficiency Video Coding (HEVC) Standard", *IEEE Transactions on Circuits and Systems for Video Technology*, vol. 22, pp. 1649–1668, 2012 (https://doi.org/10.1109/TCSVT.2012.2221191).

[31] Ch.B.A. Wael *et al.*, "Leveraging 3GPP Features and Optimization Techniques for 5G NR-V2X Resource Allocation: A Survey", *IEEE Open Journal of Intelligent Transportation Systems*, vol. 6, pp. 967–994, 2025 (https://doi.org/10.1109/OJITS.2025.3584024).

[32] M.G. Koziri *et al.*, "Efficient Cloud Provisioning for Video Transcoding: Review, Open Challenges and Future Opportunities", *IEEE Internet Computing*, vol. 22, pp. 46–55, 2018 (https://doi.org/10.1109/MIC.2017.3301630).

Anton Sorokun, Ph.D., Assoc. Professor
Department of Computer Sciences
https://orcid.org/0000-0001-8469-641X
E-mail: anton_sorokun@edu-iosa.org
State University of Information and Communication Technologies, Kyiv, Ukraine
https://duikt.edu.ua/en/

Yurii Zadontsev, Ph.D., Assoc. Professor
Department of Software Engineering
https://orcid.org/0009-0007-2192-4746
E-mail: y.zadontsev@duikt.edu.ua
State University of Information and Communication Technologies, Kyiv, Ukraine
https://duikt.edu.ua/en/

Dmytro Chyrva, Ph.D., Assoc. Professor
Department of Technical Information Protection
https://orcid.org/0009-0008-5116-5119
E-mail: dmytro.chyrva@npp.kai.edu.ua
State University "Kyiv Aviation Institute", Kyiv, Ukraine

Mykyta Zhyzhkin, Ph.D. Student
Department of Software Engineering
https://orcid.org/0009-0001-3878-6227
E-mail: 5211581@stud.kai.edu.ua
State University "Kyiv Aviation Institute", Kyiv, Ukraine

Andrii Bondarenko, Ph.D. Student
Department of Internet Technologies
https://orcid.org/0009-0007-7493-4294
E-mail: a.bondarenko@stud.duikt.edu.ua
State University of Information and Communication Technologies, Kyiv, Ukraine
https://duikt.edu.ua/en/